Design and Optimization of a Self-Inductive Displacement Sensors Based on LC Resonant Circuit

Gong Lei
School of Electrical and Control Engineering
Shaanxi University of Science and Technology
Xi'an, China
gong_lei@sust.edu.cn

Wang Xingyu
School of Electrical and Control Engineering
Shaanxi University of Science and Technology
Xi'an, China
240611010@sust.deu.cn

***Abstract*—This study, a differential self-inductive displacement sensor based on LC resonant circuit is proposed for high-precision rotor position detection in active magnetic levitation bearing systems. The relationship between the air gap variation and the inductive characteristics is analyzed by establishing an equivalent magnetic circuit model, and a differential structure is used to suppress the nonlinear error. The finite element simulation shows that the sensor has linear output characteristics in the measurement range of 0-0.9 mm with a sensitivity of 43.6 V/mm. The innovative introduction of the LC parallel resonant measurement circuit improves the sensitivity by 79.1% compared with the traditional bridge method, while maintaining excellent anti-interference and thermal stability. Experimental validation shows that the sensor exhibits a linear sensitivity of 1.45 mH/mm in the range of 0-0.4 mm, root-mean-square error of 0.0013 mH, with a maximum inductance change rate of 138%. The design provides a reliable solution for micron-level displacement detection in magnetic bearing systems, meeting the demand for precision control of high-speed rotors.**

Keywords—displacement sensor, parallel resonance, magnetic bearing

I. INTRODUCTION

The core advantage of magnetic bearings, as an efficient bearing system based on electromagnetic force to realize rotor levitation, is the significant reduction of mechanical friction. Compared with traditional bearings, magnetic levitation bearings have significant features such as frictionless, lubrication-free, long-life, pollution-free, and actively controllable [1]-[3], and are widely used in turbo-molecular pumps, machine tool spindles, blowers and compressors, etc. [4]. In the magnetic levitation bearing system, the core function of the controller is to regulate the magnetic levitation bearing coil current according to the real-time acquired rotor position signal, so as to realize the stable levitation of the rotor. Therefore, the accurate acquisition of the rotor position signal is the key element for the stable operation of the magnetic levitation bearing system. At present, the mainstream displacement detection methods in the magnetic levitation bearing system can be divided into two categories: self-sensing displacement sensors and non-contact displacement sensors. Among them, although the self-sensing technology can improve the system integration, simplify the structure and reduce the cost of equipment, its performance is seriously dependent on the accuracy of the parameters of the magnetic levitation bearing and processing precision, and the system robustness is poor, so it is difficult to meet the needs of large-scale industrial applications. In view of this, modern advanced magnetic levitation bearing systems generally use non-contact displacement sensors for rotor displacement detection. At present, the commonly used non-contact displacement sensors at home and abroad include optical displacement sensors, capacitive displacement sensors, eddy current sensors and inductive displacement sensors, etc. Optical displacement sensors and capacitive displacement sensors are susceptible to the interference of dust and dirt due to the high environmental cleanliness requirements, and their application scenarios are somewhat limited. interference, the application scenarios are somewhat limited [5]. In contrast, eddy current sensors and inductive displacement sensors have been more widely used in magnetic levitation bearing systems. It is worth noting that inductive displacement sensors have more significant advantages than eddy current sensors: they are more resistant to interference, less susceptible to external magnetic fields, and have the advantages of high sensitivity, wide measurement range, high signal-to-noise ratio, low cost, and long signal transmission distance [6], which make inductive displacement sensors have superior applicability in the detection of the rotor position in high-precision magnetic bearing systems [7].

Currently, there are many scholars at home and abroad have researched on self-inductive displacement sensors, Wang [7] designed a differential self-inductive displacement sensor for the miniaturization requirements of displacement sensors, which increased the detection range of the sensor and improved the sensitivity and linearity of the sensor, Z Ren [8] proposed a modeling method considering the magnetic resistance of the iron core and the amount of leakage, which supplemented the relevant studies on the influence of the eddy current effect and the excitation frequency on the performance of the sensor, and Wang Chunyi proposed a method for considering the magnetic resistance of the iron core and the amount of leakage. related studies on the effect of eddy current effect and excitation frequency on the performance of the sensor, Wang Chunyi [9] proposed a constant flux displacement sensor, which effectively improves the ability of the sensor to overcome the external magnetic field and improves the sensitivity of the sensor, Tang Hongzhou [10] proposed an inductive displacement sensor based on LC parallel resonance, which improves the sensitivity of the sensor and meets the requirement of higher accuracy, Chen Xinwei [11] by introducing the complex permeability of the iron core and the air-gap magnetoresistance stray coefficient, the The modeling method based on mode and impedance angle is proposed to improve the accuracy of model modeling.

The measurement circuit is an important part of the sensor design process, which serves to convert the inductance change of the sensor into a current signal that responds to the

displacement of the rotor shaft. In order to address the problem that the traditional model of self-inductive displacement sensor cannot accurately predict the sensor performance, this paper adopts theoretical derivation, finite element simulation and experimental validation to study the influence of the sensor structure parameter on the sensor performance parameters, and to explore the measures to improve the performance of the sensor.

II. Principle of Self-inductive Displacement Sensors

A. Structure of Displacement Sensors

The basic working principle of the radial self-inductive displacement sensor is that when the rotor shaft moves up and down, the air gap between the armature and the rotor shaft changes, causing changes in the magnetic circuit of the reluctance to change, resulting in a change in the inductance of the coil, so that by measuring the change in inductance in the coil can be calculated by the amount of displacement of the rotor shaft. At the same time, in order to reduce the nonlinear relationship between the sensor output signal and the air gap as well as to suppress the output error generated by temperature drift, the differential structure shown in Figure 1 is often used.

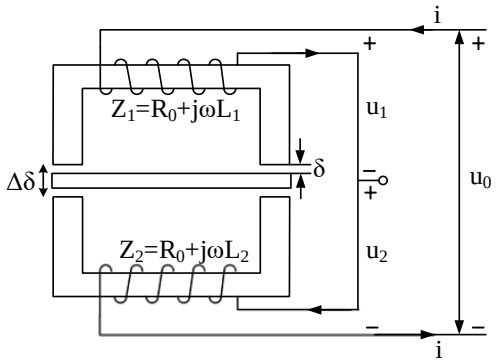

Fig. 1. Differential inductive sensor

B. Displacement Sensor Principle

From the definition of inductance and the Ohm's theorem for magnetic circuits, the expression for the self-inductance of a one-sided coil is:

$$L = N^2 / R_m \tag{1}$$

Assuming that the air gap between the stator and the rotor shaft of the sensor is much smaller than the length of the magnetic poles, and that the vacuum permeability is much smaller than the magnetic permeability of the iron core, the expression for the magnetic reluctance of the one-sided magnetic circuit is:

$$R_m = \frac{2\delta}{\mu_0 A_0} \tag{2}$$

Where: μ0 is the vacuum permeability; A0 is the air gap magnetic circuit cross-sectional area; δ is the air gap length.

Bringing (2) into (1) yields:

$$L = \frac{\mu_0 A_0 N^2}{2\delta} \tag{3}$$

From (3), it can be seen that when the number of turns of the coil is unchanged, changes in both δ and A0 can lead to changes in the inductance L. Therefore, inductive sensors can be divided into two types: variable displacement and variable air gap, and this paper mainly adopts variable air gap inductive sensors for design and analysis. Therefore, when the radial displacement Δδ occurs in the rotating shaft, the inductance of the upper and lower core coils respectively becomes:

$$\begin{cases} L_1 = \dfrac{\mu_0 A_0 N^2}{2(\delta - \Delta\delta)} = \dfrac{L_0}{1 - \dfrac{\Delta\delta}{\delta}} \\ L_2 = \dfrac{\mu_0 A_0 N^2}{2(\delta + \Delta\delta)} = \dfrac{L_0}{1 + \dfrac{\Delta\delta}{\delta}} \end{cases} \tag{4}$$

Where: L1 is the upper coil inductance; L2 is the lower coil inductance; L0 is the equilibrium position of the upper and lower coil inductance.At the same time, the amount of change in self-inductance of the upper and lower coils and the amount of change in self-inductance during differential operation is:

$$\begin{cases} \Delta L_1 = L_1 - L_0 = L_0 \dfrac{\Delta\delta}{\delta} \dfrac{1}{1 - \dfrac{\Delta\delta}{\delta}} \\ \Delta L_2 = L_2 - L_0 = -L_0 \dfrac{\Delta\delta}{\delta} \dfrac{1}{1 + \dfrac{\Delta\delta}{\delta}} \\ \Delta L = L_1 - L_2 = 2L_0 \dfrac{\Delta\delta}{\delta} \dfrac{1}{1 - \left(\dfrac{\Delta\delta}{\delta}\right)^2} \end{cases} \tag{5}$$

Then, since the sensor excitation current frequency often reaches tens of kHz, ignoring the coil resistance, the output voltage of the sensor is:

$$\Delta U = \frac{L_1 - L_2}{L_1 + L_2} U_0 \tag{6}$$

According to (5) and (6) the sensor sensitivity K is obtained as:

$$K = \frac{\Delta U}{\Delta\delta} = \frac{U_0}{\delta} \tag{7}$$

III. Finite Element Analysis of Sensors

The coil inductance is solved using Ansys software to calculate the trend of coil inductance with rotor displacement and the output characteristics of the sensor under the influence of fringing effect, eddy current effect and magnetic leakage.

A. Analysis of coil inductance variation characteristics

According to the design principle of self-sensing displacement sensor, this paper adopts the 8-pole structure of the sensor as shown in Fig. 2 as the research object, under the NSSN arrangement, during the rotation of the rotary axis, the magnetic line of force is changed less times in one cycle, and the loss is smaller, at the same time, in order to ensure the consistency of the upper and lower coils energized time sequence, the coils of the same direction are connected in series, i.e., four coils are connected in series in the Y-axis positive direction and Y-axis negative direction, four coils are connected in series in the X-axis positive direction and X-axis negative direction. The X-axis positive and X-axis negative four coils are connected in series, and the specific structural parameters are shown in Table 1.

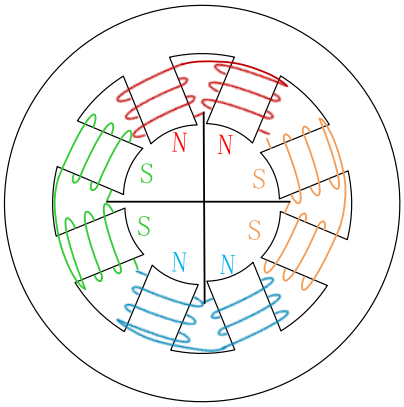

Fig. 2. Structure of an 8-pole self-inductive displacement sensor

TABLE I. STRUCTURAL PARAMETERS OF SELF-INDUCTIVE DISPLACEMENT SENSOR

Parameters	Value
δ/mm	1.0
D/mm	44.2
D_0/mm	46.2
D_1/mm	72
D_2/mm	88
A_0/mm^2	24
f/kHz	20

Since the sensor has a high degree of symmetry, this paper discusses the trends of the sensor output voltage, coil current, and coil inductance values using only the Y-axis forward displacement of 0-0.9 mm as the analyzed variables.

TABLE II. SIMULATED VALUE OF COIL SELF-INDUCTANCE

Δδ/mm	L_1/mH	L_2/mH
0.00	1.79	1.79
0.05	1.86	1.73
0.10	1.93	1.68
0.15	2.01	1.63
0.20	2.10	1.58
0.30	2.31	1.49
0.40	2.58	1.42
0.60	3.09	1.27
0.80	4.53	1.18
0.90	6.09	1.14

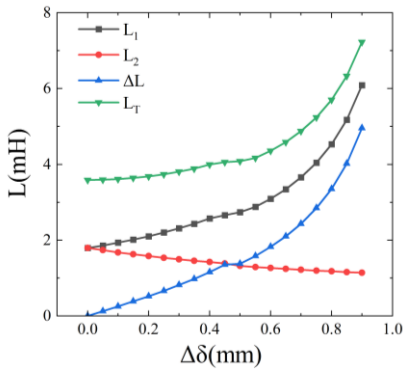

Fig. 3. Trend of simulated coil self-inductance

Table 2 shows the simulation data of coil inductance variation with rotor displacement, and the trend of coil inductance variation is plotted as shown in Fig. 3. From Table 2 and Fig. 3, it can be seen that with the increase of rotor displacement, inductances L_1, L_2, the difference of self-inductance between the upper and lower coils ΔL as well as the total self-inductance L_T all increase with the increase of rotor displacement. In the range displacement of 0-0.5 mm, the inductors L_1, L_2 and ΔL are linearized, and the total inductance L_T remains basically unchanged; in the range displacement of 0.5-0.9 mm, L_1 shows a nonlinear increase, which leads to a nonlinear increase in ΔL as well as L_T, and the maximum change in L_1 is 240%.

B. Characterization of sensor outputs

The finite element analysis yields the relationship between the sensor output voltage and the amount of displacement change as shown in Table 3 and Figure 4. According to Fig. 4, there is a good linear relationship between the sensor output voltage and the amount of displacement change, and the sensor sensitivity K=43.6V/mm.

TABLE III. SIMULATED VALUE OF OUTPUT VOLTAGE

Δδ/mm	ΔU_y/V
0.00	0.00
0.05	1.95
0.10	3.92
0.15	5.91
0.20	7.90
0.30	11.94
0.40	16.11
0.60	24.37
0.80	33.78
0.90	39.23

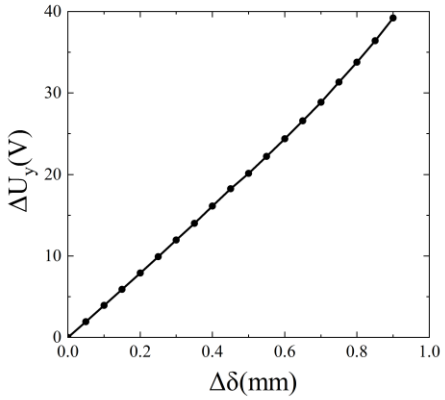

Fig. 4. Trend of simulated output voltage

IV. MEASUREMENT CIRCUIT DESIGN

As shown in Fig. 5, in order to obtain the rotor displacement signal, a measurement circuit is used to convert the rotor displacement signal into a DC signal. The measurement circuit consists of the following three parts: part 1 is the excitation circuit, which provides a stable AC excitation signal to the coil; part 2 is the modulation circuit, which converts the rotor displacement into a voltage or current

signal; part 3 is the signal conditioning circuit, which adjusts the modulation signal into a DC voltage signal proportional to the rotor displacement, where IDS+ and IDS- stand for the series-connected upper and lower coils, respectively.

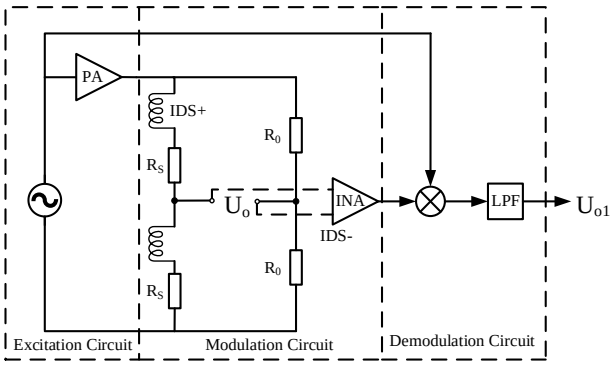

Fig. 5. Measurement circuit architecture

For the measurement of the inductance change of the sensor, a bridge circuit is usually used, which is simple and highly accurate. In order to obtain the rotor displacement signal from the modulating signal Uo, it is necessary to demodulate it. Assuming that the output voltage $U_o=U_{om}cos(\omega t+\theta)$ and the carrier $U_c=U_{cm}cos(\omega t)$, a high-frequency component and a straight current component can be obtained after passing through a multiplier：

$$\begin{aligned} U_o U_c &= U_{om}\cos(\omega t+\theta)U_{cm}\cos(\omega t) \\ &= \frac{1}{2}U_{om}U_{cm}\left[\cos(2\omega t+\theta)+\cos\theta\right] \end{aligned} \tag{8}$$

After filtering the high frequency component by a low-pass filter, the DC component can be obtained:

$$U_{ol} = \frac{1}{2}U_{om}U_{cm}\cos\theta \tag{9}$$

To further improve the sensitivity of the sensor, the focus of this paper is to improve the modulation circuit in the measurement circuit, which is a key factor in realizing high-precision position detection. Traditionally, the modulation circuit uses a differential bridge circuit to obtain the sensor signals; in this study, an LC resonant element is added to the differential bridge circuit and connected in parallel with the differential bridge arm as shown in Fig. 6.

To simplify the analysis, the LC resonant circuit is equivalent to a resistor and an inductor in series, the LC resonant equivalent circuit impedance can be expressed as:

$$Z = \frac{R_s + j\omega L_s}{\left(1-\omega^2 L_s C_p\right)+j\omega R_s C_p} = R_{eq} + j\omega L_{eq} \tag{10}$$

Since the power supply frequency is high, R_s can be neglected and the equivalent inductance is:

$$L_{eq} = \frac{L_s}{1-\omega^2 L_s C_p} \tag{11}$$

Assuming that ΔL_s is much smaller than L_s, then when the coil inductance is changed by ΔL_s and the resonance frequency is close to the excitation frequency, the relationship between the magnitude of the rate of change of the equivalent inductance and the rate of change of the coil inductance can be obtained as follows:

$$\left|\Delta L_{eq} / L_{eq}\right| > \left|\Delta L_s / L_s\right| \tag{12}$$

Therefore, the addition of the LC resonant element increases the rate of change of the equivalent inductance in the circuit, which improves the sensitivity of the modulation circuit, and then it is obtained by finite element simulation and MATLAB analysis that the LC resonant circuit increases the sensitivity by about 79.1% compared to the conventional resonant circuit. Thus, the output voltage of the modulating circuit based on LC resonance can be expressed as：

$$\begin{aligned} U_0 &= \left[\frac{R_{eq}+j\omega\left(L_{eq}+\Delta L_{eq}\right)}{R_0+R_{eq}+j\omega\left(L_{eq}+\Delta L_{eq}\right)} - \frac{R_{eq}+j\omega\left(L_{eq}-\Delta L_{eq}\right)}{R_0+R_{eq}+j\omega\left(L_{eq}-\Delta L_{eq}\right)}\right]U_i \\ &\approx \frac{\Delta L_{eq}}{L_{eq}}U_i \end{aligned} \tag{13}$$

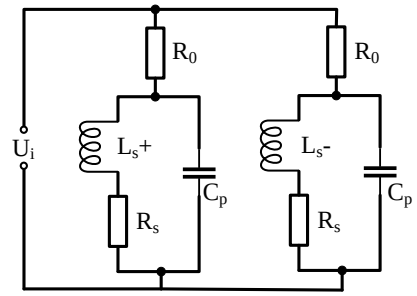

Fig. 6. LC resonant circuit

V. Experimental Verification

In order to test the inductance change characteristics and output characteristics of the self-inductive displacement sensor designed in this paper, the inductance change test rig is designed. As shown in Fig. 7, the rotor position is changed by the calibration stage, and the impedance analyzer IM3570 is used to measure the sensor coil inductance under different positions.

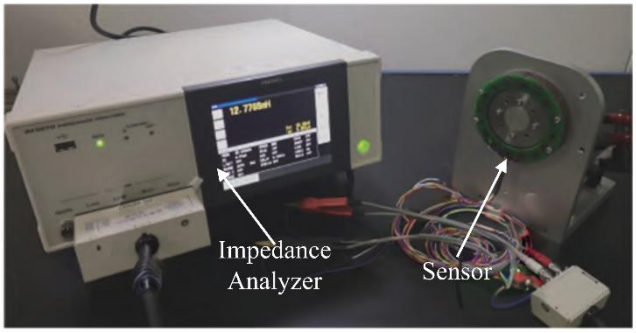

Fig. 7. Experiment rig.

Next, the output characteristics of the LC resonant circuit are analyzed by taking the inductance values of L_1 and L_2 at 0mm as the reference inductance and calculating the rate of change of the inductance; the output voltage of the circuit is calculated in accordance with (13), and then the linearity is analyzed by the root-mean-square error (RMSE), and the smaller the RMSE is, the better the linearity is. The analyzed results are shown in Fig. 8. The LC resonant circuit shows good linearity in the range of 0-0.4 mm, with a sensitivity K=1.45mH/mm, RMSE is 0.0013mH, and a maximum inductance change rate of 138%.

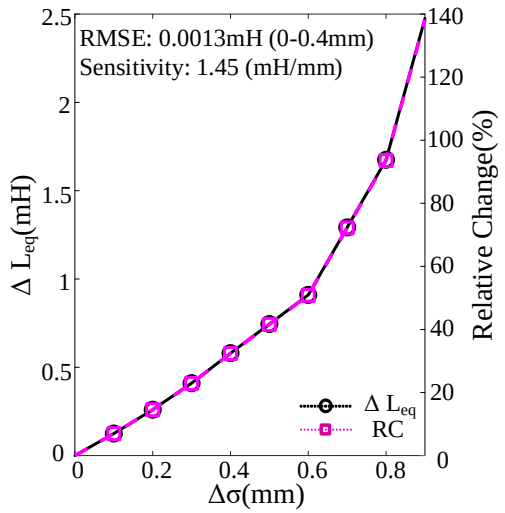

Fig. 8. Sensor output characteristic curve

VI. Conclusion

In this study, a differential self-inductive displacement sensor design based on LC resonance is proposed through the establishment of an equivalent magnetic circuit model and finite element simulation verification. The differential structure effectively suppresses the nonlinear error caused by the air gap variation, and achieves linear output in the range of 0-0.9 mm with a sensitivity of 43.6 V/mm. The innovative introduction of the LC parallel resonant measurement circuit increases the sensitivity by 79.1% compared with that of the traditional bridge circuit, and the impedance analysis experimentally verifies the linear sensitivity of 1.45 mH/mm in the range of 0-0.4 mm (RMSE=0.0013 mH). The sensor has excellent performance in terms of anti-interference and thermal stability, providing a reliable solution for micrometer displacement detection in magnetic bearing systems. Experimental data show that its maximum inductance change rate reaches 138%, which meets the demand for precision control of high-speed rotors.

References

[1] I. Royo-Silvestre, J. J. Beato-Lopez and J. C. Castellano-Aldave, *et al*., "Thrust actuator with passive restoration force for wide gap magnetic bearings," in *J. Magn. Magn. Mater.*, vol. 476, pp. 342-348, Apr. 2019.

[2] T. Soni, J. K. Dutt, and A. S. Das, "Parametric stability analysis of active magnetic bearing supported rotor system with a novel control law subject to periodic base motion," in *IEEE Trans. Ind. Electron*., vol. 67, no. 2, pp. 1160-1170, Feb. 2020.

[3] K. Wang, X. Ma and Q. Liu, *et al.*, "Multiphysics global design and experiment of the electric machine with a flexible rotor supported by active magnetic bearing," in *IEEE/ASME Trans. Mechatronics*, vol. 24, no. 2, pp. 820-831, Apr. 2019.

[4] J. Hu, W. Li and Z. Su et al., "Radial displacement measurement method for magnetic bearing based on FPC coils," in *IEEE Sens. J.*, vol. 24, no. 19, pp. 29687-29694, Oct. 2024.

[5] W. Xiong, W. Sun and K. Liu, *et al.*, "Research progress of active magnetic suspension technology for high-speed motorized spindles,"in *J. Mech. Eng*., vol. 57, no. 13, pp. 1-17, Apr. 2021.

[6] C. Jin, Z. Ye and J. Zhou, *et al*., "Design and analysis of transverse flux sensor for magnetic bearings," in *J. Instrum*., vol. 44, no. 9, pp. 228-238, Jan. 2023.

[7] K. Wang, L. Zhang and Y. Le *et al.*, "Optimized differential self-inductance displacement sensor for magnetic bearings: Design, analysis and experiment," in *IEEE Sens. J*., vol. 17, no. 14, pp. 4378-4387, Jul. 2017.

[8] Z. Ren, H. Li and X. Chen *et al.*, "Impedance modeling of self-inductive displacement sensor considering iron core reluctance and flux leakage," in *IEEE Sens. J.*, vol. 22, no. 9, pp. 8583-8595, May , 2022.

[9] C. Wang, Y. Xu, and K. Zhang, "Parameter study of axial inductive displacement sensor with constant flux for magnetic bearings,"in *J. Vib. Meas. Diagn*., vol. 43, no. 6, pp. 1095-1102+1242, Dec. 2023.

[10] H. Tang, J. Zhou, C. Jin, *et al*., "Design of axial self-inductive displacement sensor based on LC parallel resonance,"in *J. Zhejiang Univ. (Eng. Sci.)*, vol. 58, no. 5, pp. 1072-1079, Mar. 2024.

[11] X. Chen, H. Li and Z. Ren, *et al*., "Impedance modeling of self-inductive displacement sensor based on mode and impedance angle," in *Trans. China Electrotech. Soc.*, vol. 40, no. 2, pp. 387-397, Jan. 2025.